A New Antenna Array and Signal Processing Concept for an Automotive 4D Radar

Martin Stolz[#1], Maximilian Wolf[#2], Frank Meinl[#3], Martin Kunert[#4], Wolfgang Menzel[*#5]

[#]Advanced Engineering Sensor Systems, Robert Bosch GmbH Leonberg

[*]Institute of Microwave Techniques, Ulm University

[1]martin.stolz2@de.bosch.com, [5]wolfgang.menzel@uni-ulm.de

***Abstract* — On the way to Highly Automated Driving (HAD), new conditions for sensors used in vehicles arise. To achieve a highly accurate environmental perception the resolution of radar sensors has to be increased. Only with fine grained sensor information, it is possible to maneuver safely and highly automated at all road conditions in urban and rural surroundings. A prototypical implementation of such a sensor, which fulfills all these requirements, is presented in the following as automotive 4D radar. The relevant parts of the baseband signal processing are explained in combination with the used modulation waveform. A new antenna array arrangement is introduced which provides the ability to measure angles in both azimuth and elevation. To estimate the two angles of arrival a method which performs this in combination is exemplified. First measurements with a cyclist are recorded and show a radial speed enhanced 3D radar image. The first results are extremely promising. For validation of the measured data, also a simulation of the same scenario with identical system parameters is performed and shown.**

***Keywords* — automotive radar, signal processing, angular estimation, 2d angular estimation.**

I. Introduction

The evolution from innovative driver assistance systems for more safety and comfort, over partially automated driving systems towards highly automated driving (HAD), is a big challenge in today's automotive research and development area. One of the main tasks is an accurate capturing of the environment around the moving vehicle. With today's sensor generations used in Advanced Driver Assistance Systems (ADAS) like Adaptive Cruise Control (ACC) or Automatic Emergency Braking Systems (AEB), a first development step is done. To deliver adequate information about the surrounding for use in HAD applications the sensor performance has to be improved [1], [2].

Radar is awarded a key role on the way to automated driving [3]. Among others, radars are independent from environmental conditions (darkness, weather), are able to directly measure the distance and Doppler velocity and have a multiple field of view capability. Furthermore the Micro-Doppler effect in radar [4] enables the classification of pedestrians, cyclists (Vulnerable Road Users, VRU's) and vehicles according to their characteristic velocity spread [5], [6].

A first experimental radar sensor system [7], is already in use and shows promising results in measurement accuracy and classification of VRU's. In future Highly Automated Driving vehicles one class of sensor systems is not sufficient. A combination of automotive sensors based on different physical principles (e.g. camera, lidar and radar), is currently rated as most effective [8]. To get a basis for the fusion of the sensor detections on pixel level, the radar sensor performance has to be improved towards higher resolution imaging.

In order to be able to detect objects in three-dimensional space with a radar sensor system, a 2D antenna array is needed. The additional information, compared to an on market automotive radar sensor, is used to enhance the classification of VRU's, recognize under- and over runnable objects and percept the environment more accurately.

The presented 4D radar are able to measure objects in the three spatial directions (x, y and z) and the associated radial velocity component.

The organization of the paper is as follows. In Section II a short review of the used radar platform is given. A new antenna array design is presented, the underlying signal model is described and the signal processing for the angle estimation of the two angles (azimuth and elevation) is shown in Section III - V. At last radar images based on simulated and measured data are shown in Section VI.

II. Brief Review of the used Radar Platform

The following is a brief overview of the used radar system platform described in [7]. One part consists of the RF-Frontend with additional baseband signal processing and AD-conversion. It works in the $76\,\mathrm{GHz}$ to $81\,\mathrm{GHz}$ automotive frequency band with fast chirp, linear FMCW ramps. The sensitivity of the system is high enough to detect objects in more than $100\,\mathrm{m}$ distance and with an accuracy of about $6\,\mathrm{cm}$. Object velocity detection is up to $\pm 20\,\mathrm{m/s}$ with a resolution of $4\,\mathrm{cm/s}$. The second part is completely digital and includes a FPGA-processing platform with extension modules for raw data transfer between the two components. In the FPGA design the very first signal processing steps, namely FIR filtering, two dimensional spectrum transformation by FFT and ordered-statistics (OS) CFAR are processed. Due to the spatial separation of the two sensor parts, it is easy to change parts, for example the radar frontend. For the novel automotive imaging radar a 2D planar antenna array is designed for this platform.

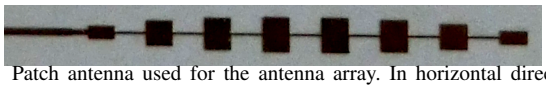

Fig. 1. Patch antenna used for the antenna array. In horizontal direction is elevation and in vertical direction is azimuth.

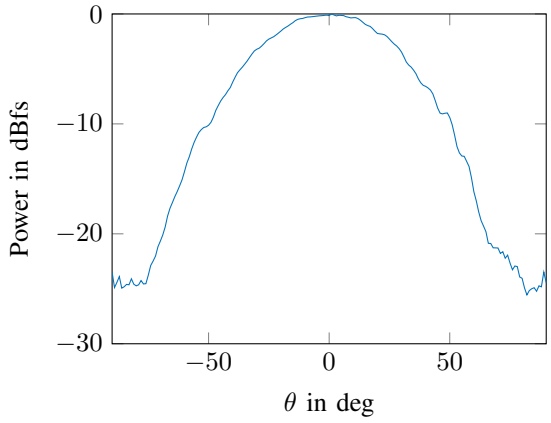

(a) azimuth

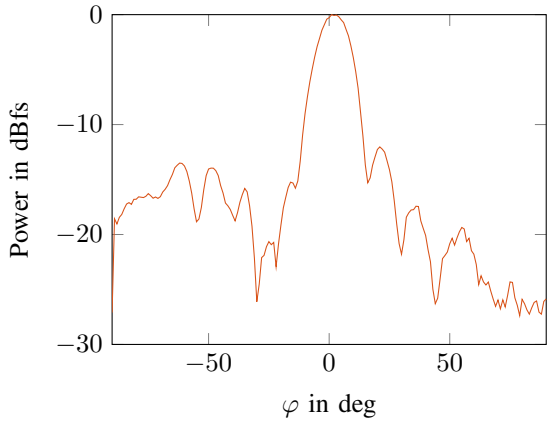

(b) elevation

Fig. 2. Normalized two way antenna pattern in azimuth and elevation.

III. Antenna Array Design

Two requirements have been made for the antenna array design. To capture objects in a wide detection range, a wide field of view in azimuth direction is required. To meet this requirement, an antenna is used which is designed as a series-fed patch array which consists of eight patch elements. The realized antenna is shown in Fig. 1. To check if the opening angle of the used antenna meets the requirement and for characterization, the two way antenna pattern is measured and shown in e-plane and h-plane for azimuth and elevation in Fig. 2. It shows a wide field of view in azimuth direction and a smaller field of view in elevation direction.

The second requirement is to detect objects in three-dimensional Cartesian space with one transmitting antenna. In order to fulfill this requirement it is necessary to detect the distance as well as the two angles in azimuth and elevation of the object. Distance detection with a fast chirp linear FMCW radar is described in [9]. To detect the two angles, an antenna array is required with distribution

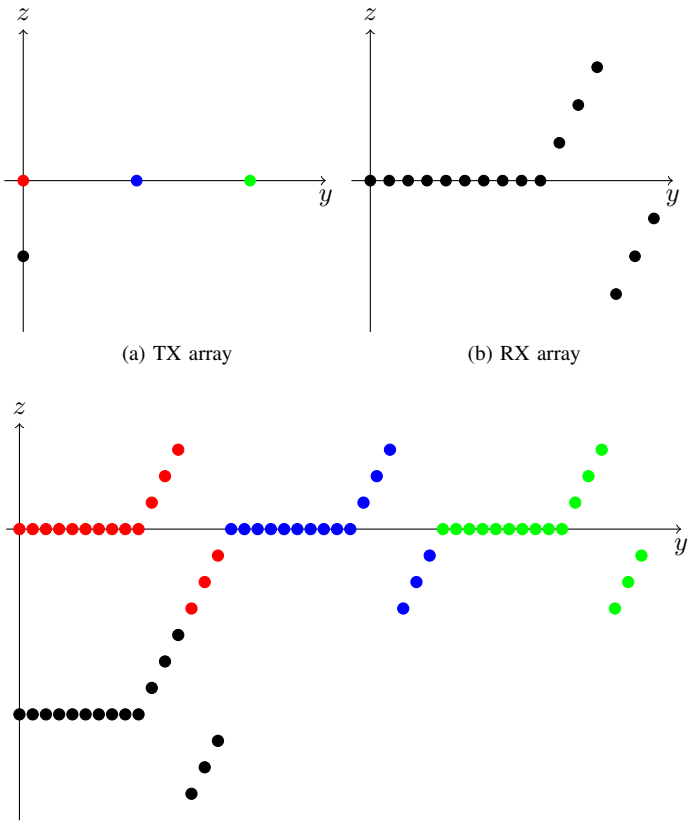

(a) TX array (b) RX array

(c) Virtual array

Fig. 3. MIMO array design with the transmitting array in (a), the receiving array in (b) and the corresponding virtual array in (c).

of the receiving antenna elements in two dimensions. The presented array is designed as a Multiple Input Multiple Output (MIMO) array [10] with 4 transmitting elements and 16 receiving elements, to get the ability of enlarging the aperture of the array in azimuth and elevation. The array of the transmitting, receiving and corresponding virtual antenna channels is shown in Fig. 3. The arrangement of the array elements is influenced by the size of the series-fed patch antenna. Along the y-axis an uniform array element spacing of $0.7\,\lambda$ is used. In z-direction the array elements are uniformly spaced with a distance of λ.

IV. Signal Model

For the given antenna array the 16 received signals can be expressed as

$$\boldsymbol{y}(t) = \boldsymbol{A}\boldsymbol{s}(t) + \boldsymbol{n}(t) \tag{1}$$

where $\boldsymbol{y}(t) = \left[y_0(t), \ldots, y_N(t)\right]^T$ is the vector of the received signals, $\boldsymbol{s}(t) = \left[s_1(t), \ldots, s_K(t)\right]^T$ is composed by K signals reflected from objects, $\boldsymbol{n}(t) = \left[n_1(t), \ldots, n_N(t)\right]^T$ is the additive white Gaussian noise (AWGN) and the superscript T denotes the transpose operation. The array manifold matrix of narrowband sources is described by

$\boldsymbol{A} = \left[\boldsymbol{a}(\theta_1, \varphi_1), \ldots, \boldsymbol{a}(\theta_K, \varphi_K)\right]$ and characterized by the two angles θ (azimuth) and φ (elevation) for each object. In $\boldsymbol{a}(\theta, \varphi) = \left[e^{-jkP_1\boldsymbol{D}^T}, \ldots, e^{-jkP_N\boldsymbol{D}^T}\right]^T$ the phase difference between the antenna elements dependent on θ and φ are described. In $P = \left[(x_1, y_1, z_1), \ldots, (x_N, y_N, z_N)\right]^T$ the three dimensional Cartesian coordinate points of the N antenna elements are given. The wave number $k = (2\pi)/\lambda$ is a constant factor, with $\lambda = c_0/f_c$, the wave propagation speed c_0 in vacuum and the carrier frequency f_c. With $\boldsymbol{D} = \left[\cos(\theta)\cos(\varphi), \sin(\theta)\cos(\varphi), \sin(\varphi)\right]$ the direction of the spherical coordinate system of the radar system is defined. Thus, the received signals are completely described.

V. 2D Angular Estimation

For the angle estimation of the two angles θ and φ, a robust and fast technique was looked for. The conventional beamformer was selected, which is also referred to as Bartlett beamformer [11]. This algorithm maximizes the power of the beamforming output for a given input signal. The classical spatial spectrum is obtained by

$$P_{BF}(\theta) = \frac{\boldsymbol{a}^H(\theta)\boldsymbol{y}(t)\boldsymbol{y}^H(t)\boldsymbol{a}(\theta)}{\boldsymbol{a}^H(\theta)\boldsymbol{a}(\theta)} \tag{2}$$

and only defined for one angle θ. The superscript H denotes the hermitian operator which conjugates and transposes the matrix. It is easy to extend the approach to two angles by

$$P_{BF}(\theta, \varphi) = \frac{\boldsymbol{a}^H(\theta, \varphi)\boldsymbol{y}(t)\boldsymbol{y}^H(t)\boldsymbol{a}(\theta, \varphi)}{\boldsymbol{a}^H(\theta, \varphi)\boldsymbol{a}(\theta, \varphi)}. \tag{3}$$

To find the maximum of the spatial spectrum each combination of the two angles has to be performed. This needs a high processing effort. To decrease the processing load the spatial spectrum is calculated in a different way. First the normalization of the magnitude of the steering vector $\boldsymbol{a}(\theta, \varphi)$ to one is done in a pre-processing step, so the denominator of (3) is always one and can be neglected. To find the maximum of the spatial spectrum only the complex magnitude is used. This allows a representation of the spatial spectrum as

$$A_{BF}(\theta, \varphi) = \left|\boldsymbol{y}^H(t)\boldsymbol{a}(\theta, \varphi)\right|^2. \tag{4}$$

By replacing $\boldsymbol{a}(\theta, \varphi)$ with the array manifold matrix $\boldsymbol{A_M}(\theta, \varphi)$ with all possible combinations of the two angles θ and φ in between the region of interest, (4) becomes the discrete cross correlation function

$$\boldsymbol{A}_{BF}(\theta, \varphi) = \left|\boldsymbol{y}^H(t)\boldsymbol{A_M}(\theta, \varphi)\right|^2. \tag{5}$$

It is possible to completely process the angle estimation within one matrix multiplication. For the generation of the manifold matrix, it is possible to use theoretically generated data or data obtained by calibration. Furthermore, in radar systems multiple objects have to be estimated per measurement cycle. Therefore $\boldsymbol{y}(t)$ has to be replaced by $\boldsymbol{Y}(t) = \left[y_1(t), \ldots, y_K(t)\right]$ which contains the K detected objects per measurement cycle.

$$\boldsymbol{A}_{BF}(\theta, \varphi) = \left|\boldsymbol{Y}^H(t)\boldsymbol{A_M}(\theta, \varphi)\right|^2 \tag{6}$$

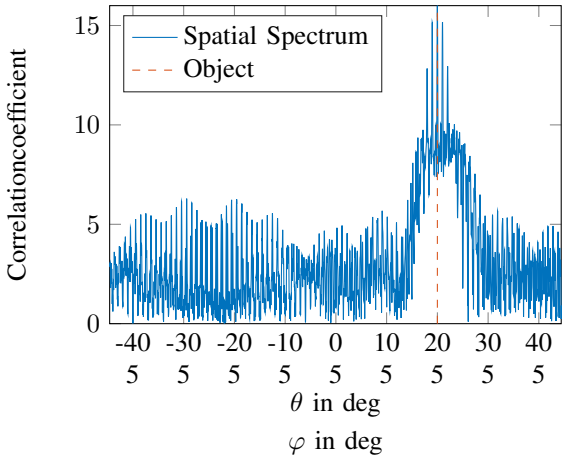

Fig. 4. Spatial spectrum of the combined angle estimation of θ and φ.

To find the estimated angles of each object the maximum value of the rows in $\boldsymbol{A}_{BF}(\theta, \varphi)$ is needed. With the combined array manifold matrix for θ and φ, the indices of the maximum row values indicates both angles of each detected object. An example of the spatial spectrum is shown in Fig. 4. For clarity, the index was plotted along the horizontal axis into its two constituents in θ and φ. It is not only used $\varphi = 5\,^\circ$, rather φ is in the area between $\pm 30\,^\circ$ and θ between $\pm 45\,^\circ$. The detected object is located at $\theta = 20\,^\circ$ and $\varphi = 5\,^\circ$. With the proposed method the maximum of the spatial spectrum is at the position corresponding to the angles of the object.

VI. Radar Imaging

With the collected informations of the range r, radial velocity v_r and the two angles θ and φ of an object, described in the previous parts, full 4D radar images can be generated. In this case, three dimensions are according to the three spatial directions (x, y and z) and the fourth dimensions according to the radial velocity v_r. To transform r, θ and φ into x, y and z the following equation is used

$$\begin{bmatrix} x \\ y \\ z \end{bmatrix} = r \begin{bmatrix} \cos(\theta)\cos(\varphi) \\ \sin(\theta)\cos(\varphi) \\ \sin(\varphi) \end{bmatrix}. \tag{7}$$

This transformation is used for each detection of the radar. By plotting these detections in a three dimensional Cartesian coordinate system and colouring the points dependent on v_r, a complete radar image in 4D appears. A simulated example of such an image with the described radar parameters of section II, is shown in Fig. 5. The image shows a cyclist crossing from the left side to the right side. The wheels of the bicycle can be recognized very well by the typical round shape and the distribution of the velocity [12].

The same scenario is measured with the real radar system and the result is plotted in Fig. 6. Similar to the simulated radar image, it is also easy to recognize the wheels of the bicyclist. Difference in the distribution of the radial velocity, for instance at the wheels occurs from a slightly change of the trajectory in the real world measurement to the right hand side. Thereby the

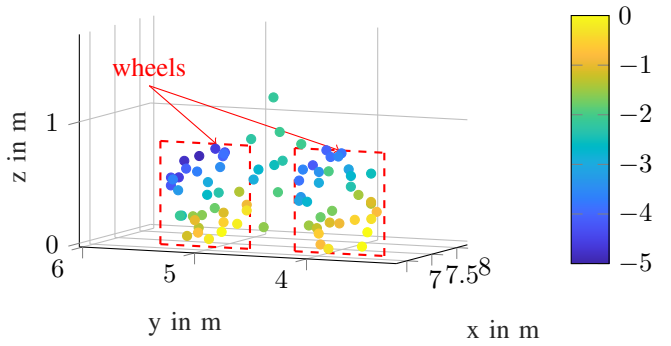

Fig. 5. Radar image of a simulated cyclist with detection points position in (x,y,z) and coloured radial velocity in m/s.

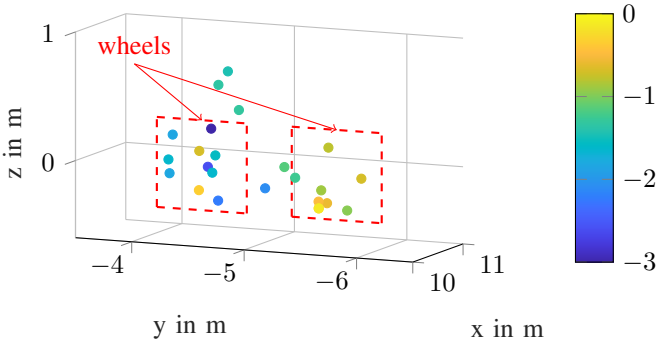

Fig. 6. Radar image of a real cyclist measurement with detection points position in (x,y,z) and coloured radial velocity in m/s.

perspective varies and the radial velocity components change, which makes a great impact at the low speeds of the cyclist. Another variation between the two images is the number of the detection points. The synthetic data are created without any consideration of multi-path propagation, only additive white Gaussian noise is used. In the real world measurements some different kind of noise occurs, also multi-path propagation and dependent on the radar perspective more or less different radial velocity values. To separate detection points, in our case different radial velocities are important.

VII Conclusions

This paper shows a way to generate a 4D radar image. Starting with the introduction of the used prototype radar platform, with focus on real time baseband signal processing. Furthermore a new 2D planar antenna array design is introduced which enables the detection of the two angles θ and φ for a three dimensional object detection. Also the two way antenna pattern in e-plane and h-plane is pointed out. Estimation of the two angles within one algorithm is shown under consideration of the underlying signal model. As additional information to the three dimensional detection points, the radial velocity is taken into account. With these informations first multi-dimensional radar images are shown with both, measurement and simulation data. They show promising results and quality for further work. With such kind of measurements, it is possible to achieve a detailed representation of the environment and additionally a classification of the detected road users. With such environmental perception capabilities, Highly Automated Driving comes closer.

Acknowledgment

The research leading to the results of this work has received funding from the European Community's Eighth Framework Program (Horizon2020) under grant agreement n° 634149 for the PROSPECT project. The PROSPECT consortium members express their gratitude to the European Commission for selecting and supporting this project.

References

[1] J. Hasch, "Driving towards 2020: Automotive radar technology trends," in *Microwaves for Intelligent Mobility (ICMIM), 2015 IEEE MTT-S International Conference on*, April 2015, pp. 1–4.

[2] J. Dickmann, J. Klappstein, M. Hahn, M. Muntzinger, N. Appenrodt, C. Brenk, and A. Sailer, "Present research activities and future requirements on automotive radar from a car manufacturer's point of view," in *Microwaves for Intelligent Mobility (ICMIM), 2015 IEEE MTT-S International Conference on*, April 2015, pp. 1–4.

[3] J. Dickmann, J. Klappstein, M. Hahn, N. Appenrodt, H. L. Bloecher, K. Werber, and A. Sailer, "Automotive radar the key technology for autonomous driving: From detection and ranging to environmental understanding," in *2016 IEEE Radar Conference (RadarConf)*, May 2016, pp. 1–6.

[4] V. C. Chen, F. Li, S. S. Ho, and H. Wechsler, "Micro-doppler effect in radar: Phenomenon, model, and simulation study," *IEEE Transactions on Aerospace and Electronic Systems*, vol. 42, no. 1, pp. 2–21, Jan 2006.

[5] S. Heuel and H. Rohling, "Pedestrian classification in automotive radar systems," in *Radar Symposium (IRS), 2012 13th International*, May 2012, pp. 39–44.

[6] E. Schubert, F. Meinl, M. Kunert, and W. Menzel, "High resolution automotive radar measurements of vulnerable road users - pedestrians & cyclists," in *Microwaves for Intelligent Mobility (ICMIM), 2015 IEEE MTT-S International Conference on*, April 2015, pp. 1–4.

[7] F. Meinl, M. Stolz, M. Kunert, and H. Blume, "An experimental high performance radar system for highly automated driving," in *IEEE MTT-S 2017 International Conference on Microwaves for Intelligent Mobility*, 2017.

[8] F. Kunz, D. Nuss, J. Wiest, H. Deusch, S. Reuter, F. Gritschneder, A. Scheel, M. Stbler, M. Bach, P. Hatzelmann, C. Wild, and K. Dietmayer, "Autonomous driving at ulm university: A modular, robust, and sensor-independent fusion approach," in *2015 IEEE Intelligent Vehicles Symposium (IV)*, June 2015, pp. 666–673.

[9] C. Schroeder and H. Rohling, "X-band fmcw radar system with variable chirp duration," in *Radar Conference, 2010 IEEE*, May 2010, pp. 1255–1259.

[10] J. Li and P. Stoica, *MIMO Radar Signal Processing*. New York: John Wiley & Sons, 2008.

[11] H. Krim and M. Viberg, "Two decades of array signal processing research: the parametric approach," *Signal Processing Magazine, IEEE*, vol. 13, no. 4, pp. 67–94, Jul 1996.

[12] M. Stolz, E. Schubert, F. Meinl, M. Kunert, and W. Menzel, "Multi-target reflection point model of cyclists for automotive radar," in *2017 European Radar Conference (EURAD)*, Oct 2017, pp. 94–97.